Liquid Crystals
Publication details, including instructions for authors and subscription information:
http://www.informaworld.com/smpp/title~content=t713926090

DNA liquid crystalline blue phases. Electron microscopy evidence and biological implications

Amélie Leforstier[a]; Françoise Livolant[a]
[a] Laboratoire de physique des Solides, Bat 510, Université Paris Sud, Orsay, Cedex, France

To cite this Article Leforstier, Amélie and Livolant, Françoise(1994) 'DNA liquid crystalline blue phases. Electron microscopy evidence and biological implications', Liquid Crystals, 17: 5, 651 — 658
To link to this Article: DOI: 10.1080/02678299408037336
URL: http://dx.doi.org/10.1080/02678299408037336

LIQUID CRYSTALS, 1994, VOL. 17, NO. 5, 651–658

DNA liquid crystalline blue phases
Electron microscopy evidence and biological implications

by AMÉLIE LEFORESTIER and FRANÇOISE LIVOLANT*
Laboratoire de physique des Solides, Bat 510, Université Paris Sud,
91405 Orsay Cedex, France

(*Received 14 January 1994; accepted 1 March 1994*)

The isotropic–liquid crystalline transition of concentrated DNA solutions is investigated using freeze–fracture electron microscopy in order to understand the first steps of the DNA condensation process. Between the isotropic liquid and the cholesteric mesophase, we report the existence of double twist DNA bundles and describe their long range ordering into 3D networks. This organization corresponds to the formation of 'blue phases' already observed in thermotropic liquid crystals, but never reported in lyotropic systems. In addition, the size of the DNA molecule, about ten times that of most thermotropic materials, allows here the molecular resolution imaging of blue phase structures. Since such structures recall chromatin organization of some Procaryotes and lower Eucaryotes, we suspect that they may be widespread and of potential interest in the regulation of chromatin functions.

1. Introduction

The understanding of chromatin organization as well as that of DNA condensation and decondensation processes still remains an outstanding question. In addition to the effect of specialized proteins, the spontaneous ordering of DNA into liquid crystalline phases that occur at high concentration [1–6] has to be taken into account as a leading mechanism in chromatin packaging. Indeed, the cell nucleus is a macromolecular crowded medium, both ordered and fluid, where the DNA concentration is locally in the range 50 to 500 mg ml^{-1} [7, 8]. Liquid crystalline DNA therefore represents a convenient model by which to mimic the close approach of double helices during chromatin condensation by a simple increase of polymer concentration.

Concentrated DNA solutions form lyotropic liquid crystals the nature of which depends on the polymer concentration. Two phases are known so far: a cholesteric phase [1, 2, 9] and a columnar hexagonal phase [5, 10–12]. The isotropic–cholesteric phase transition is usually first order as seen by polarizing microscopy: cholesteric germs nucleate and grow amidst the isotropic liquid [13, 14] and finally merge into a homogeneous cholesteric phase. With 50 nm DNA fragments, this transition occurs around 130 mg ml^{-1} [4, 6]. With longer fragments (50 nm to 3 μm), a second order transition was also observed and analysed [15]). We focus here on the isotropic–cholesteric transition to understand the first stages of DNA condensation at the molecular level. Freeze–fracture electron microscopy allows the precise visualization

* Author for correspondence.

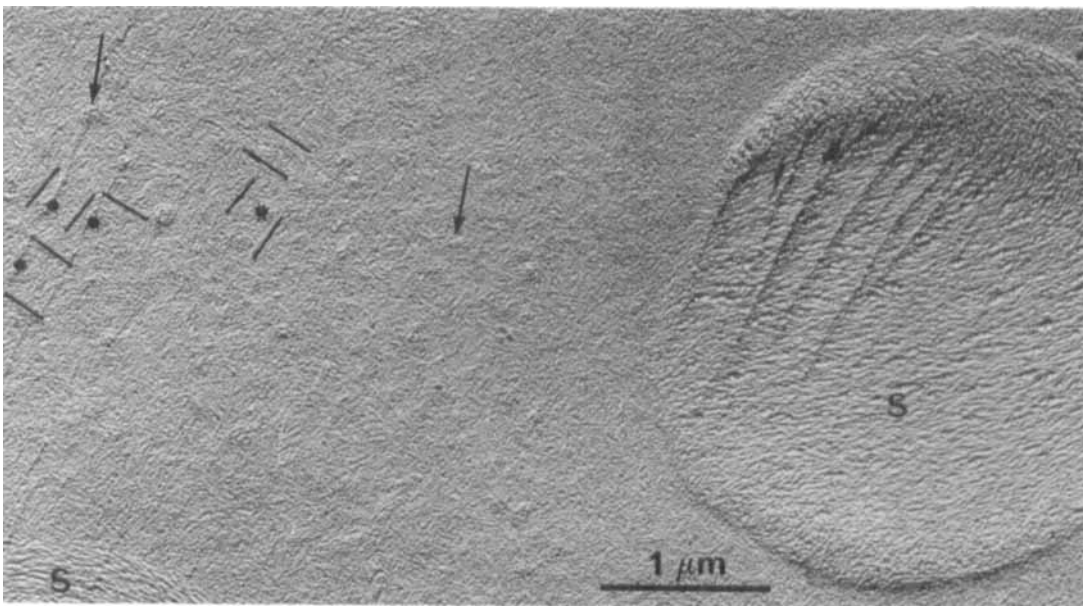

Figure 1. Freeze–fracture-etch electron microscopy of concentrated DNA solution at the transition between the isotropic and the cholesteric phases. Around the spherulites (S), one observes clustered DNA bundles (arrows) that appear regularly aligned parallel or perpendicular to the fracture plane, as respectively underlined by dashes and knots, thus drawing quasi-periodic-like patterns (bar = 1 μm).

of molecular orientations and is therefore an accurate tool to analyse this transition at the molecular level.

2. Experimental

Sample preparation: Short-length DNA fragments (about 50 nm, figures 2 and 4 (*a*)) were obtained by selective digestion of calf thymus chromatin with micrococcal nuclease according to the method described in [41] while longer fragments (50 to 5000 nm, figures 1 and 3 (*b*)) were obtained by sonication at 0°C of commercial calf thymus DNA (Merck) dissolved in 5 mM Tris (pH 8) at a concentration of 1 mg ml^{-1}. After precipitation in ethanol, the DNA was air-dried and dissolved in 0·25 M-ammonium acetate, 10 mM-sodium cacodylate, 0·5 mM-EDTA (pH 7·0) or in NaCl 0·25 M, 10 mM-sodium cacodylate, 0·5 mM-EDTA (pH 7·0) at a concentration of about 100 mg ml^{-1} a few days to a month before performing the experiments.

Electron microscopy: Drops of DNA solution were deposited onto copper discs and were allowed to concentrate by slow evaporation of the solvent, until they reached the phase transition concentration (cholesteric spherulites in equilibrium with the isotropic liquid). In order to check the state of the samples at any time, DNA droplets were observed in parallel by polarizing microscopy.

Solutions of short-length DNA fragments were then allowed to stabilize in a humid atmosphere during 1 to 24 h to obtain homogeneous samples; there was no stabilization in a humid atmosphere of solutions of long molecules.

Samples were quickly frozen by projection on to a copper block cooled down to

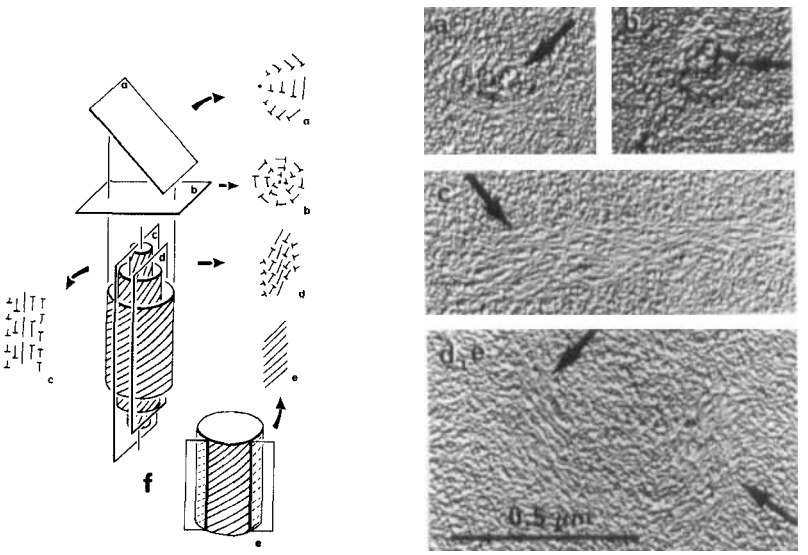

Figure 2. Geometrical analysis of the DNA bundles observed by freeze-etch electron microscopy. The different aspects of DNA bundles observed at high magnification (bar = 0·5 μm) (*a*, *b*, *c*, *d*, *e*) can be interpreted as different fracture planes through a double twist cylinder of DNA molecules (*f*). In the double twist structure, there exists a twist angle between neighbouring molecules in any direction in space normal to their elongation axis. Molecular orientations follow helical paths that can be conveniently drawn upon a series of concentric cylinders of increasing size, even though the real structure is continuous. Transverse fracture planes of the cylinder (plane *b*) raise circular patterns with molecules oblique to the fracture plane at the periphery and normal in the centre. According to the nail convention, molecular orientations in projection on to the plane of observation are represented by lines, nails and points when molecules respectively lie parallel, oblique and normal to the section plane. Oblique fracture planes (plane *a*) raise elliptic patterns. Along the small axis of the section, molecular orientations vary from parallel to normal to the fracture plane when moving from one side of the bundle to the other. Fracture planes parallel to the bundle axis produce elongated patterns. Depending on the level of fracture inside the bundle, these patterns, display either unidirectional (*c*) or sigmoidal (*d*) molecular arrangements. In some cases, the fracture plane more or less follows the surface of the bundle instead of sectioning it, showing molecular alignments oblique to the bundle elongation axis (*e*). All the expected patterns were recognized on the freeze–fracture replicas and labelled the same way; note that *d* and *e* patterns cannot always be distinguished.

10 K by liquid helium in a cryovacublock device (Reichert, after Escaig [40] and immediately transferred into liquid nitrogen. Fracture was performed at -110°C under a 2×10^{-7} Torr vacuum; this sample was etched at -100°C for 2 to 4 min, platinum–carbon shadowed at an angle of 45° and carbon coated (Balzers BAF 400T). After washing in distilled water, replicas were observed in a 201 Philips TEM at 40 or 60 kV accelerating voltage.

3. Results and discussion

3.1. *Double twist cylinders*

Cholesteric spherulites can be recognized in section on freeze fracture replicas observed in the electron microscope (see figure 1, S). Yet, we shall not deal here with

these germs, but focus rather on the space between them. Careful examination of the medium surrounding the cholesteric spherulites reveals numerous heterogeneities that correspond to small, clustered DNA bundles (see figure 1, arrows). The occurrence of the phenomenon seems to be restricted to a sharp concentration range at the isotropic–cholesteric transition, since more dilute solutions simply display homogeneous aspect that corresponds to the true isotropic liquid (not illustrated).

At high magnification, the molecular orientations can be followed precisely, allowing the 3D structure of the bundles to be decided: the different observed patterns (see figures 2 (*a*)–(*d*)) can be interpreted as different possible sections of a double twist cylinder as sketched in figure 2 (*f*). Within these small cylindrical domains, DNA assumes a double twist ordering, i.e. there exists a twist angle between neighbouring molecules in any direction in space normal to the molecular long axis (whereas twist occurs in a single direction in the cholesteric phase).

Measurement of the diameter and thickness of the bundles allows their description as small cylinders, 40 to 200 nm in width and up to 800 nm in length. The angle α of the molecular direction at the surface of the cylinder can reach a maximum value of 45° relative to the axis of the bundle (see figure 2 (*d*)). Molecular orientations therefore undergo a 45° rotation over about 100 nm. The helical pitch, corresponding to a 360° rotation of molecular orientations, would therefore equal 800 nm. The average twist angle between neighbouring molecules can be estimated from the helical pitch and the inter-helix spacing within the structure. If we assume the latter value as close to 4·9 nm (as measured at the isotropic–cholesteric transition by Durand *et al.* [16]), it is thus possible to conclude that each double twist cylinder contains 8 to 40 DNA molecules tilted on average at about 1·8°, one relative to another. This is significantly different from the molecular twist in the cholesteric phase, typically in the range of 0·7–0·8° (calculated after Van Winkle *et al.* [17], Durand *et al.* [16], and Leforestier and Livolant [9]).

3.2. *Long-range ordering of the double twist cylinders*

In addition to this local molecular order, one may now consider the long range ordering of the double twist cylinders themselves. There exist two main situations that can be related to the degree of space occupancy of cylinders that are more or less densely packed in an area under consideration:

(1) On the one hand, the double twist tubes form loose networks whose occupancy varies continuously from 10–15 to 50 per cent of the space, the inter-space being isotropic (see figure 3 (*a*)). These networks do not display any long range order. Yet, locally, within the lowest tube density areas (up to about 25 per cent), there exist domains where, on average, some tubes tend to align more or less parallel (weak nematic-like order). Some at least of these tubes happen to be connected. As their density increases, a faintly discernible random network, with more connections between the double twist cylinders, appears (not illustrated).

(2) On the other hand, the double twist tubes (whose diameter now varies only from 80 to 150 nm) fill the entire space. They can no longer be easily picked out individually and one observes somewhat intricate patterns (see figures 1 and 3 (*b*)). These dense networks are long range ordered: the cylinders alternatively orient along three main directions (underlined in figure 3 (*b*)). This regular alternation changes progressively, raising a wide variety of patterns which lack

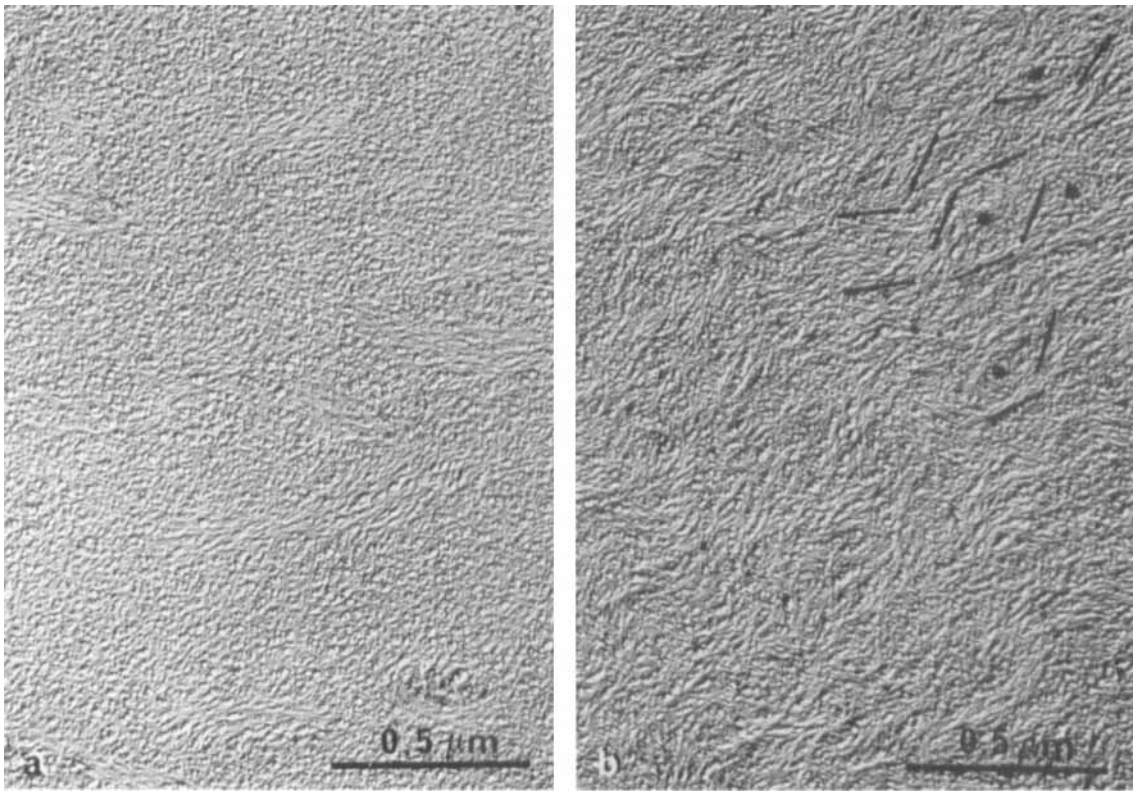

Figure 3. Long-range order: different networks of double twist cylinders corresponding to short-length DNA fragments (50 nm, (*a*)) and longer ones (50 to 5000 nm, (*b*)) (bar = 0·5 μm). (*a*) The bundles are separated one from another by the isotropic solution and can be followed individually. They do not exhibit a preferential orientation, though, locally, some tend to align more or less in parallel. (*b*) Complex network of double twist bundles that alternatively follow three different main orientations, probably orthogonal to one another in space (see also figure 1). The network fills the entire space and the unit bundles are difficult to individualize.

true periodicity. These quasi-periodic patterns in the plane imply a true periodic 3D network [18, 19], probably cubic. We estimate the distance between two cylinders of similar orientation in space to be in the range of 300 nm.

The high reproducibility of these observations, as well as the long-range order of the dense networks precludes the hypothesis of transient pretransitional fluctuations. In addition, these structures are not induced by the freezing process, since the vicinity of the cholesteric germs is usually devoid of such bundles. Besides, less concentrated solutions prepared in the same way never display these patterns. Moreover, double twist bundles are well known to be the basic building blocks of the three blue phases that form in very narrow temperature ranges between the isotropic and the cholesteric phases of chiral thermotropic liquid crystal materials. Our observations can hereby be related to blue phase formation in a narrow concentration range. As far as we know, blue phases have not yet been detected in lyotropic polymer systems, but there is no a priori reason for their occurrence to be ruled out.

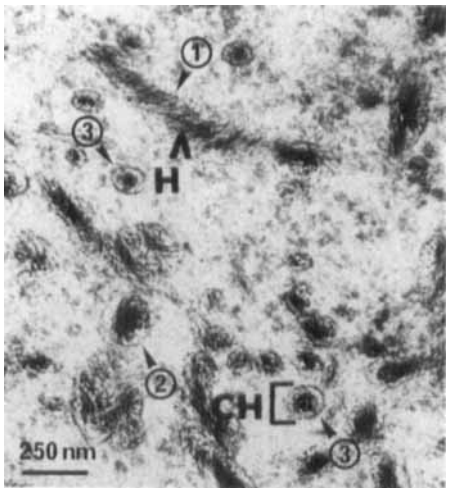

Figure 4. Electron microscopic observation of a section through a nucleus of the Dinoflagellate *Peridinium cinctum* at the peak of ^{3}H thymidine uptake (replication stage). The unwound chromosomes (CH) show different aspects similar to those presented in figure 2, that we interpret as different orientations of the section plane relative to the axis of a double twisted chromatin structure: nearly parallel (1), oblique (2) and normal (3). Moreover, this section is thick enough to observe the hair-lock aspect of the chromatin filaments within the bundle (bar = 250 nm). Picture kindly provided by Dr D. L. Spector.

The structure and symmetry properties of blue phases were developed mainly within the framework of the Landau phase transition theory [20–23] which explains the possible occurrence of three different blue phases (BP I, BP II and BP III) at the transition between the isotropic and the cholesteric phase. We have observed here at least two of them. The first one corresponds to a loose random network of double twist cylinders, which is consistent with the spaghetti model of BP III [24, 25]. This phase, that has hitherto been described as macroscopically amorphous, while locally highly ordered, still remains somewhat enigmatic. Three main models have been proposed: (i) the *spaghetti* model as a spaghetti-like tangle of double twist cylinders [24, 25], (ii) the cubic domain model in which double twist tubes form local small cubic domains that are randomly oriented relative to one another [20, 26] and (iii) the quasi-crystal model that abides by an icosahedral symmetry [22, 27].

DNA solution could provide an accurate tool to further investigations of this enigmatic BP III structure. Indeed, our observations not only support the spaghetti model, but also allow one to specify it. Some additional features are already available, in particular those related to the manner of space filling by the tubes, namely continuous density variations of tubes and connections between cylinders. We may in particular wonder whether structural discontinuities do occur at a given density threshold, beyond which the network would be connected, hence involving the hypothesis of space percolation.

As regards the second blue phase, it could be either BP I or BP II (cubic arrays of double twist tubes, body centred cubic and simple cubic, respectively [21, 28, 29]). As already pointed out, a precise determination of the lattice parameters would require further 3D reconstruction from the electron microscopy

data, together with diffraction studies of the samples over a large range of wavelengths.

Though electron microscopic imaging of thermotropic blue phases has already been reported in literature [30–34], such a visualization of the local molecular order within the double twist cylinder of blue phases was hitherto precluded, because of the small size of thermotropic mesogens. The level of resolution under discussion here allows us to draw comparisons with chromatin organization *in vivo*. Convincing evidence of blue phase-like ordering can be observed on micrographs of some Dinoflagellate nuclei (*Peridinium cinctum*) obtained by Spector *et al.* [35] and reproduced here in figure 4. This state corresponds to the replication stage of the genetic material that leads to a physiological decondensation of chromosomes [35] which are usually cholesteric [13, 36]. We suspect such an organization to be widespread in Prokaryotes. For example, according to the species and the physiological state of the cell, bacterial nucleoids display multiple aspects, ranging from typically condensed cholesteric to fully dispersed [37–39]. For the intermediate levels of compaction, micrographs suggest the presence of such double twist configurations that nonetheless still remain to be studied in detail.

Since it is now well established that DNA condensation stimulates the functional properties of the molecule *in vitro*, we may suspect the geometrical supramolecular configurations of the DNA molecule to be involved in regulation processes. The spontaneous ordering of DNA into double twist structures, that appears as a general feature of the first stages of DNA supramolecular ordering (this work and also [15]), could indeed fulfil *in vivo* some particular requirements of the genetic material to be in a given functional state.

Dr D. L. Spector is deeply acknowledged for allowing us to reproduce a micrograph of *Peridinium cinctum*. This work was supported by a grant from INSERM (No. 910909).

References

[1] ROBINSON, C., 1961, *Tetrahedron*, **13**, 219.
[2] ROBINSON, C., 1966, *Molec. Crystals*, **1**, 467.
[3] LERMAN, L. S., 1973, *Cold Spring Harb. Symp quant. Biol.*, **38**, 59.
[4] STRZELECKA, T. E., DAVIDSON, M. W., and RILL, R. L., 1988, *Nature, Lond.*, **331**, 457.
[5] LIVOLANT, F., 1991, *J. molec. Biol.*, **218**, 165.
[6] RILL, R. L., STRZELECKA, T. E., DAVIDSON, M. W., and VAN WINKLE, D. H., 1991, *Physica A*, **176**, 87.
[7] MINTON, A. P., 1981, *Biopolymers*, **20**, 2093.
[8] DUBOCHET, J., 1993, *Trends Cell Biol.*, **3**, 1.
[9] LEFORESTIER, A., and LIVOLANT, F., 1993, *Biophys. J.*, **65**, 56.
[10] LUZZATI, V., and NICOLAIEFF, A., 1959, *J. molec. Biol.*, **1**, 127.
[11] LIVOLANT, F., and BOULIGAND, Y., 1986, *J. Phys., Paris*, **47**, 1813.
[12] LIVOLANT, F., LEVELUT, A. M., DOUCET, J., and BENOIT, J. P., 1989, *Nature, Lond.*, **339**, 724.
[13] LIVOLANT, F., 1984, *Eur. J. Cell Biol.*, **33**, 300.
[14] BOULIGAND, Y., and LIVOLANT, F., 1984, *J. Phys., Paris*, **45**, 1899.
[15] LIVOLANT, F., 1987, *J. Phys., Paris*, **48**, 1051.
[16] DURAND, D., DOUCET, D., and LIVOLANT, F., 1992, *J. Phys. II, France*, **2**, 1769.
[17] VAN WINKLE, D. H., DAVIDSON, M. W., CHEN, W. X., and RILL, R. L., 1990, *Macromolecules*, **23**, 4140.
[18] GAILL, F., and MOSSERI, R., 1990, *C. r. hebd. Séanc. Acad. Sci., Paris*, **311**, 1479.
[19] LEFORESTIER, A., and LIVOLANT, F., 1992, *J. Phys. II, Paris*, **2**, 1853.

[20] BELYAKOV, V. A., DEMIKHOV, E. I., DMITRIENKO, V. E., and DOLGANOV, V. K., 1986, *Zh. eksp. teor. Fiz.*, **89,** 2035; 1986, *Soviet Phys. JETP*, **62,** 1173S.
[21] WRIGHT, D. C., and MERMIN, N. D., 1989, *Rev. mod. Phys.*, **61,** 385.
[22] HORNREICH, R. M., and SHTRIKMAN, S., 1986, *Phys. Rev. Lett.*, **56,** 1723.
[23] HORNREICH, R. M., and SHTRIKMAN, S., 1988, *Molec. Crystals liq. Crystals*, **165,** 183.
[24] HORNREICH, R. M., KUGLER, M., and SHTRIKMAN, S., 1982, *Phys. Rev. Lett.*, **48,** 1404.
[25] KITZEROW, H. S., COOKER, P. P., and HEPPKE, G., 1991, *Phys. Rev. Lett.*, **67,** 2151.
[26] COLLINGS, P. J., 1984, *Phys. Rev.* A, **30,** 1990.
[27] ROKHSAR, D. S., and SETHNA, J. P., 1986, *Phys. Rev. Lett.*, **56,** 1727.
[28] HORNREICH, R. M., and SHTRIKMAN, S., 1981, *Physics Lett.* A, **84,** 20.
[29] MEIBOOM, S., SAMMON, M., and BERREMANN, D. W., 1983, *Phys. Rev.* A, **28,** 2553.
[30] COSTELLO, M. J., MEIBOOM, S., and SAMMON, M., 1984, *Phys. Rev.* A, **29,** 2957.
[31] ZASADZINSKI, J. A. N., MEIBOOM, S., SAMMON, M. J., and BERREMAN, D. W., 1986, *Phys. Rev. Lett.*, **57,** 364.
[32] HARA, H., SATOH, T., TOYA, T., ORII, S., and WATANABE, J., 1988, *Macromolecules*, **21,** 14.
[33] GILLI, J. M., KAMAYE, M., and SIXOU, P., 1991, *Molec. Crystals liq. Crystals*, **199,** 79.
[34] DELACROIX, H., GILLI, J. M., ERK, I., and MARIANI, P., 1992, *Phys. Rev. Lett.*, **69,** 2935.
[35] SPECTOR, D. L., VASCONCELOS, A. C., and TRIEMER, R. E., 1981, *Protoplasma*, **105,** 185.
[36] BOULIGAND, Y., SOYER, M. O., and PUISEUX-DAO, S., 1968, *Chromosoma*, **24,** 251.
[37] HOBOT, J. A., VILLIGER, W., ESCAIG, J., MAEDER, M., RYTER, A., and KELLENBERGER, E., 1985, *J. Bact.*, **162,** 96.
[38] KELLENBERGER, E., 1991, *Res. Microbiol.*, **142,** 229.
[39] KELLENBERGER, E., and ARNOLD-SCHULZ-GAHMEN, B., 1992, *FEMS Microbiol. Lett.*, **100,** 361.
[40] ESCAIG, J., 1982, *J. Microsc.*, **126,** 221.
[41] STRZELECKA, T. E., and RILL, R. L., 1987, *J. Am. chem. Soc.*, **109,** 4513.
[42] ESCAIG, J., 1982, *J. Microsc.*, **126,** 221.